

Electron spectroscopy studies of PTCDA on Ag/Si(111)- $\sqrt{3}\times\sqrt{3}$

J. B. Gustafsson,* H. M. Zhang, E. Moons, and L. S. O. Johansson
Department of Physics, Karlstad University, SE-651 88 Karlstad, Sweden

(Received 8 September 2005; revised manuscript received 20 March 2006; published 16 April 2007)

The growth of 3,4,9,10-perylene tetracarboxylic dianhydride thin films on the Ag/Si(111)- $\sqrt{3}\times\sqrt{3}$ surface has been studied by means of high-resolution photoelectron spectroscopy (PES), near edge x-ray absorption fine structure (NEXAFS) and low-energy electron diffraction (LEED). LEED and NEXAFS data indicate that for the first molecular layer there is a well ordered growth of flat lying molecules in several phases with a preferred ordering relative to the substrate. There is a clear interaction between the perylene core of the molecule and substrate seen from changes of the highest occupied molecular orbital and lowest unoccupied molecular orbital levels in the PES and NEXAFS data. Shifts in the C 1s and O 1s XPS core levels are interpreted as interactions with the carboxylic groups. There are also new components and changes in the low coverage XPS C 1s and O 1s core level spectra compared to spectra from thicker, pure molecular films. The new components can be related to two different parts of the molecule. One is located in the carboxylic groups and the other in the perylene core of the molecule. For thicker films the NEXAFS and core level results suggest a mainly layered growth of flat lying molecules.

DOI: 10.1103/PhysRevB.75.155413

PACS number(s): 73.61.Ph, 79.60.Fr, 68.55.-a

I. INTRODUCTION

Thin organic molecular films have gained an increasing attention since they have promising electronic and optical properties for potential use in electronic applications. To optimize properties such as charge transport in these films, high structural order is needed. The further structural growth is largely affected by the order of the first monolayer. A detailed understanding of the interface processes is therefore important in order to optimize organic-inorganic devices. The planar perylene derivative 3,4,9,10-perylene tetracarboxylic dianhydride (PTCDA) has been widely used as model compound for such organic molecular thin films¹ and is applied in organic optoelectronic devices such as organic light emitting diodes.¹

The film growth is mainly controlled by the relative strengths of the competing molecule-molecule and molecule-substrate interactions. Well ordered films of flat lying molecules can be formed on weakly interacting surfaces such as Au and highly oriented pyrolytic graphite.¹ On more reactive semiconductor surfaces, there is often less ordering of PTCDA molecules due to the substrate dangling bonds.^{2,3} We have earlier found that passivation of a silicon substrate enhances the film quality.^{3,4} For surfaces with intermediate interaction strength true epitaxial growth with site recognition can be found.⁵ One prominent example is Ag where the PTCDA molecules on the Ag(111) surface display a herringbone-like growth with two molecules per unit cell in commensurate layers.⁵ On the Ag(110) surface a nearly square lattice is formed with one molecule per unit cell in a brick-wall-like ordering.⁶ Nearly square unit cells are also reported for PTCDA on Au(111) and Au(100) with two molecules per unit cell rotated 90° with respect to each other.⁷

We have previously studied PTCDA on clean and hydrogen passivated Si(001)2×1. These two surfaces represent two extreme cases where the clean surface is very reactive and the H-passivated surface is inert. In this paper we present results of a study of PTCDA on the Ag/Si(111)- $\sqrt{3}\times\sqrt{3}$ sur-

face. This surface is intrinsically semiconducting,⁸ described by the honeycomb chain trimer (HCT) model with a full monolayer of Ag (Ref. 8) shown schematically in Fig. 1(a). In this model the uppermost Si atoms and the Ag atoms form trimers in the top layer. Recently a small modification of the Ag atom positions in the HCT model was proposed due to inconsistencies in low temperature scanning tunneling microscopy (STM) images.⁹ The surface is very sensitive to extra Ag, leading to higher surface conductivity and other reconstructions, even for very little extra Ag present. The

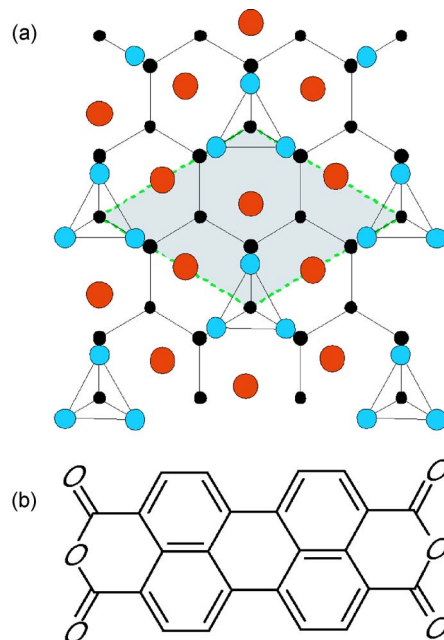


FIG. 1. (Color online) (a) The HCT model of the Ag/Si(111)- $\sqrt{3}\times\sqrt{3}$ -surface. The largest circles are positions of Ag atoms. The size of the circles indicate which layer the atoms belong to (smaller circles for lower layers). The unit cell of the substrate surface is marked. (b) The PTCDA molecule. The sizes of the molecule and substrate are in the same scale.

density of occupied states (DOS) on the surface is nonuniform and concentrated to the Ag trimers. This is in contrast to a metal surface where the DOS is nearly homogeneous.

A recent low coverage STM study of PTCDA on Ag/Si(111)- $\sqrt{3} \times \sqrt{3}$ showed several different commensurate or nearly commensurate, herringbone, square, and hexagonal phases. It was suggested that these new two-dimensional phases were stabilized by interactions with the substrate.¹⁰

STM studies of C₆₀ (Refs. 11 and 12) and pentacene¹³⁻¹⁵ on Ag/Si(111)- $\sqrt{3} \times \sqrt{3}$ showed that highly ordered molecular layers were formed. C₆₀ had preferential bonding at step edges and defect sites and further deposition leads to highly ordered islands in double domains.¹² For pentacene two different well ordered phases were formed in the submonolayer range with a significant difference in the packing density.¹³ In a PES study of pentacene on this surface a 0.35 eV interface dipole was observed.¹⁶ There was also a change in the pentacene C 1s core level lineshape from an asymmetric peak at 0.5 ML coverage gradually evolving to one symmetric peak at 4 ML film thickness indicating different adsorption sites for the molecules in the first layer.¹⁶

II. EXPERIMENTAL DETAILS

This study was made at the D1011 bending magnet beamline¹⁷ at the MAX-lab synchrotron radiation facility located in Lund, Sweden. The beamline is equipped with a Zeiss SX-700 plane-grating monochromator and with a large hemispherical electron analyzer of Scienta SES200-type. The D1011 station is also equipped with a partial-yield electron detector for near edge x-ray absorption fine structure (NEXAFS) measurements. The end station consists of separate analyzer and preparation chambers, accessible with a long-travel manipulator. The base pressures were 3×10^{-10} mbar. The measuring parameters were set up to give an energy resolution < 100 meV for the XPS measurements.

An As *n*-doped Si(111) sample (Wacker-Chemitronic) with a resistivity of 0.003 Ω cm was used as substrate. Before inserting the substrates in the UHV system the samples were chemically treated with a method described by Ishizaka and Shiraki¹⁸ to get a thin protecting oxide. The substrates were then out-gassed *in situ* by resistive heating slowly to 600 °C, where the temperature was kept for several hours. Then the oxide was removed by annealing to 940 °C for about 4 min. A low-energy electron diffraction (LEED) image of the resulting surface showed a sharp 7×7 pattern. The surface was subsequently annealed again to 940 °C for 30 s and then 3 Å of Ag was deposited monitored by a quartz crystal microbalance. This is followed by annealing in steps at 540 and 600 °C to form a $\sqrt{3} \times \sqrt{3}$ reconstruction without any excess silver on the surface.⁸

PTCDA was deposited from a home-built source, consisting of a crucible heated by a filament, while the substrate was kept at room temperature. The source was out-gassed for several hours. The deposition rate was measured with a quartz crystal microbalance to about 2 Å/min. The settings of the microbalance have previously been calibrated with atomic force microscopy and STM measurements. Stepwise PTCDA depositions were done up to 0.3, 0.6, 1, 2, and 10

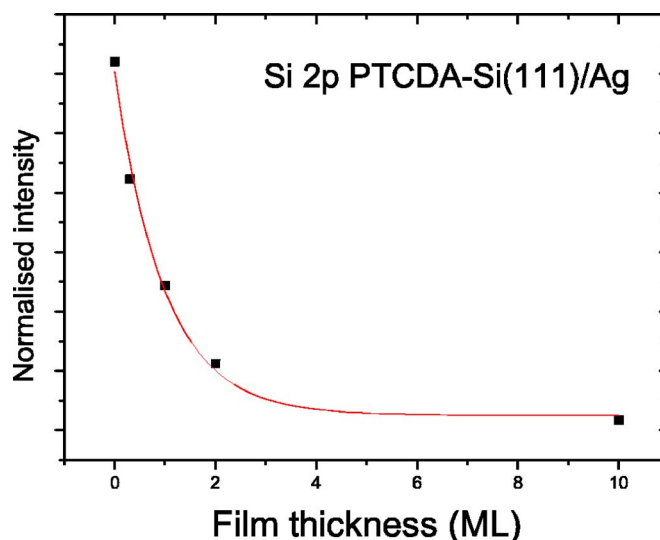


FIG. 2. (Color online) Intensity of the Si 2p XPS signal as a function of film thickness and the fitted exponential decay.

ML thicknesses. Si 2p, C 1s, O 1s core level spectra, valence band spectra and partial yield carbon *K*-edge NEXAFS spectra with 200 V retarding voltage were recorded after each growth stage. The Fermi level position was verified by photoemission measurements of a Ta foil in electrical contact with the sample. The accuracy of the absolute energy scale from the monochromator was estimated to be ± 0.5 eV.¹⁹

The work function of the sample was obtained by measuring the cutoff energy of the photoemission spectra with the sample biased by a negative voltage of 10 V. In the peak-fits the background for C 1s was reduced with a Shirley function and for O 1s with a polynomial function. A Voigt type core level shape has been used. The Lorentzian was fixed to 100 meV and the Gaussian widths were fitted in each case with the FITXPS program.

III. RESULTS

A. Silicon 2p core level

The attenuation of the substrate Si 2p signal is shown in Fig. 2 and can be fitted with an exponential decay according to the formula

$$I = I_0 e^{-t/\lambda}, \quad (1)$$

where λ is the mean free path, t is the film thickness, and I_0 and I are the Si 2p peak intensity for the bare and PTCDA covered substrate. This indicates a layer by layer growth with a mean free path of 3.2 Å in the PTCDA film. However, there are only a few data points so this conclusion is somewhat uncertain.

The Si 2p core level spectra (not shown) with PTCDA deposited show only a very small change in line shape compared to the clean Ag/Si(111)- $\sqrt{3} \times \sqrt{3}$ spectra. There is a slight shift of the main component by 0.11 eV to lower binding energy when one ML of PTCDA is deposited. As the line shape is almost unchanged we assign the same shift to the bulk component and interpret this as a small band bending

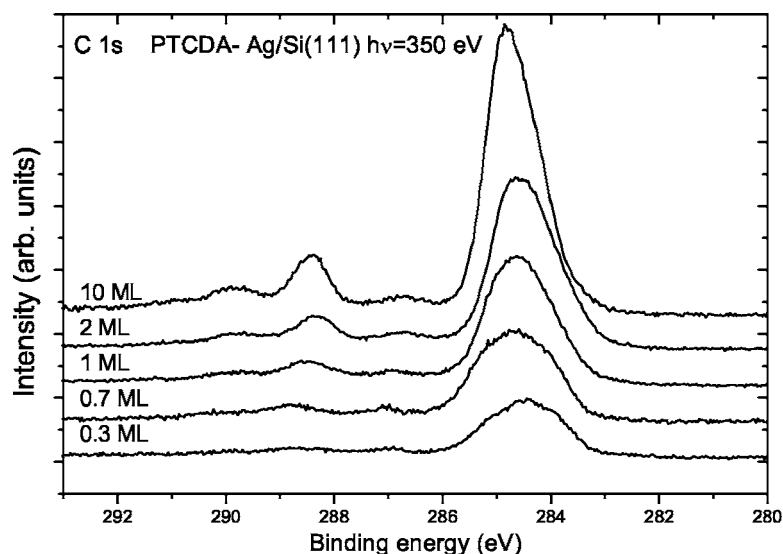


FIG. 3. Normalized C 1s core level spectra for PTCDA layers of different thickness on Ag/Si(111)- $\sqrt{3} \times \sqrt{3}$.

shift. The shifts of the Si 2p core level for different coverages are presented in Fig. 7 together with the shifts of the core levels of carbon and oxygen and will be discussed below.

B. Carbon 1s core level

C 1s XPS spectra for varying thicknesses of PTCDA are shown in Fig. 3. The spectra have two main peaks. The larger one at a binding energy of 284.8 eV is assigned to carbon in the perylene core of the molecule and a smaller one at 288.4 eV to the carboxylic group.²⁰ Fitting of the components in the C 1s spectra has been done for films with thicknesses varying from submonolayer up to 10 ML with the background reduced by an integrating Shirley function. A selection of the fits are presented in Fig. 4. It can be noted that the spectrum for a 10 ML thick film of PTCDA on Ag/Si(111) is very similar to the one for thick PTCDA films on H passivated Si(001) (Ref. 3) and Ag(111),²¹ where the components are related to the pure molecular film. We will compare the 10 ML spectrum with lower coverage spectra and point out the differences.

The main features for the C 1s spectrum for the 10 ML thick PTCDA film are the two components labeled *a* and *b* in Fig. 4 which constitute the main peak. As mentioned above this peak is assigned to the perylene core of PTCDA. It was fitted with two components in a 1.5:1 intensity ratio (a small deviation from this was allowed in the fitting process) because of an asymmetry due to the chemically different C atoms in the perylene core. Component *a* is assigned to the twelve carbon atoms with only C-C bonds and *b* to the eight atoms with a C-H bond. This assignment is supported by calculations of the atomic charges in a PTCDA molecule²² which show that the latter C atoms are negatively charged, while the twelve C atoms with only C-C bonds have no or very little charge. The smaller feature labeled *c* at 288.4 eV in the 10 ML spectrum is from the C atoms in the carboxylic groups. This assignment is based on the higher electronegativity of the O atoms giving a higher binding energy to these electrons.^{20,22} Additionally the areas of the fitted components

correspond to the stoichiometry of the molecule.

The other smaller peaks *d*, *e*, and *f* have previously been assigned to shake-up effects^{23,24,21} and our data do not provide evidence for a different assignment. Peak *d* has also previously been suggested to arise from an interaction between the anhydride group and the Si substrate for PTCDA on Si(100).²⁴ The stoichiometric ratio between the carbon atoms in the perylene core and in the end groups for a free molecule is 5:1. This is in good agreement with the 5.3:1 ratio of the integrated area of components (*a+b*):(*c+e*) from the fitted components of a 10 ML thick film where any intensity deriving from molecule-substrate interactions are strongly attenuated.

The C 1s core level spectra for thinner layers are slightly different compared to thick films. The peakfits in the submonolayer range are compared with the one for the spectrum of the 10 ML thick film and are shown in Fig. 4 with the main peak parameters summarized in Table I. The main peak is relatively similar on all coverages apart from an increased width and an extra component at 285.5 eV labeled *g* on the lower coverages. For 0.3 ML coverage the peaks related to the carboxylic group are less well defined and relatively weaker compared to the main components. The component *d* has a slightly higher intensity at this coverage compared to a thick film.

The peak *c* also appears to have a different shift of binding energy compared to the main peak. With increasing thickness from 0.3 to 2 ML the peak gets much sharper and the binding energy decreases by 0.33 eV while the main peak stays at roughly the same energy.

In the evolution of spectra from 0.3 to 10 ML a relative weakening of the *g* component at 285.2 eV and the *d* component at 286.8 eV in favor of the carboxylic group related component *e* is seen, as the thickness increases. The *g* component has its largest intensity at 0.3 ML and the weakening appears to start before a full monolayer is deposited. The *g* component is not needed to make a good fit above 1 ML coverage. The energy shifts as a function of coverage are shown in Fig. 7. In order to understand the interaction between the molecules and the substrate the differences in the

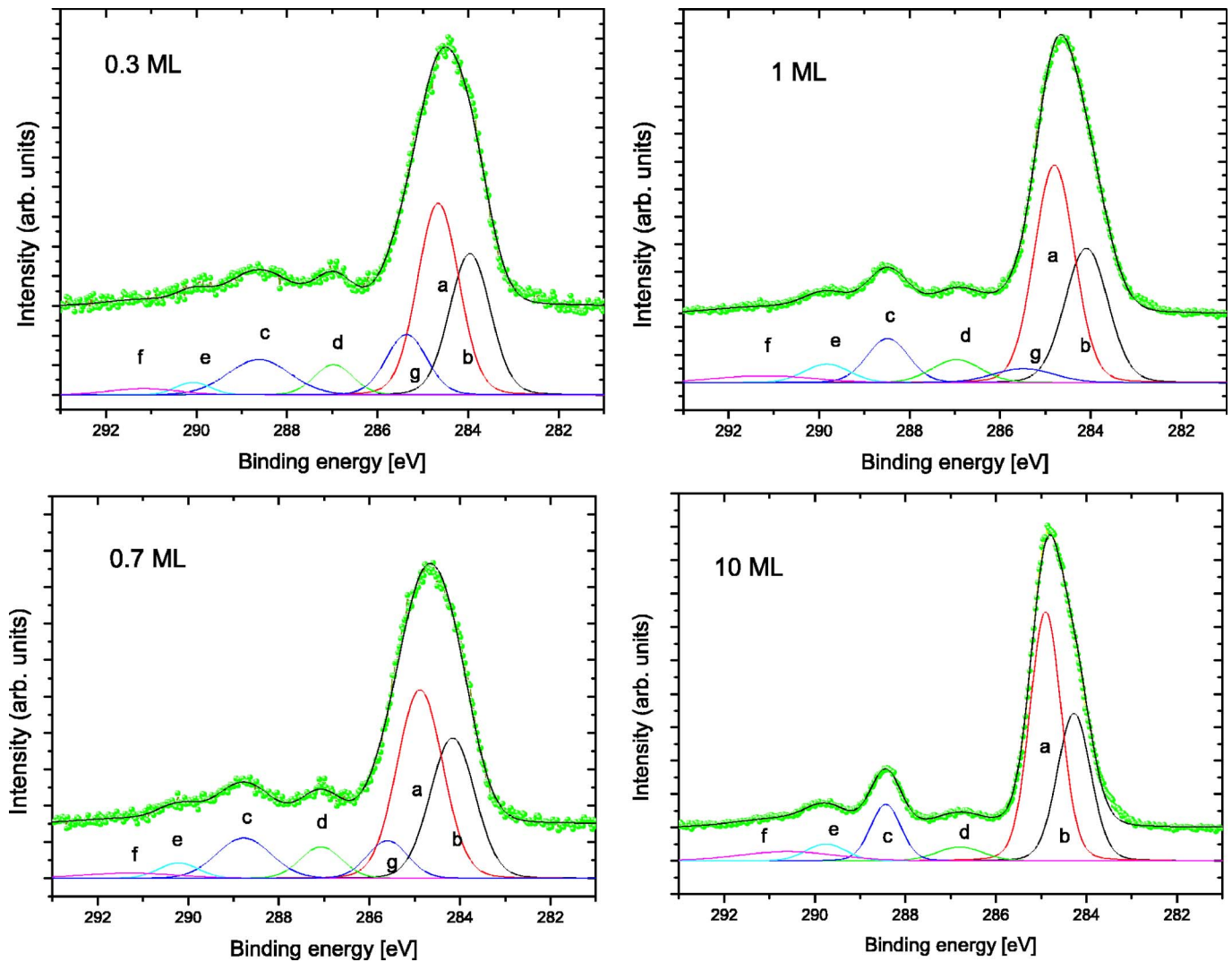


FIG. 4. (Color online) Peakfits of C 1s for various coverages of PTCDA on Ag/Si(111). Experimental data are shown as points and the fitted data with a continuous line. The fitted components are shown with continuous lines and labeled a–g.

low coverage spectra must be explained and will be discussed later together with the other XPS results.

C. Oxygen 1s core level

Similar to the C 1s spectra there is a clear thickness dependence of the O 1s core level spectra (Fig. 5). Curve fitted

spectra are shown in Fig. 6 and the fit parameters listed in Table II. For a 10 ML film the spectrum looks similar to the ones for thick films of PTCDA on Si(001)-H and Ag(111).^{4,21} The larger component at 530.55 eV labeled A has previously been assigned to the carboxylic group and component B at 532.5 eV has been assigned to the O atoms in the anhydride group.²⁰ The deviation from the expected

TABLE I. Fitting parameters for components a, b, c, d, e, and g of C 1s. The table shows the energy position ΔE relative peak a [eV], relative integrated intensity I_{rel} and FWHM W_G of the Gaussian in eV.

0.3 ML	ΔE	I_{rel}	W_G	0.7 ML	ΔE	I_{rel}	W_G	1 ML	ΔE	I_{rel}	W_G	10 ML	ΔE	I_{rel}	W_G
b	0	28.4%	1.02	b	0	29.7%	1.13	b	0	28.1%	1.00	b	0	29.6%	0.81
a	0.70	39.0%	1.01	a	0.72	40.1%	1.11	a	0.73	45.4%	0.99	a	0.63	47.0%	0.76
c	4.66	10.7%	1.58	c	4.61	10.4%	1.36	c	4.41	8.5%	1.03	c	4.16	10.3%	0.74
d	3.01	5.7%	0.93	d	2.91	6.2%	1.02	d	2.87	5.7%	1.23	d	2.52	3.8%	1.16
e	6.12	2.2%	0.81	e	6.05	3.0%	1.00	e	5.75	4.5%	1.12	e	5.48	4.0%	0.98
g	1.40	12.1%	1.00	g	1.44	7.2%	1.00	g	1.32	4.2%	1.5				

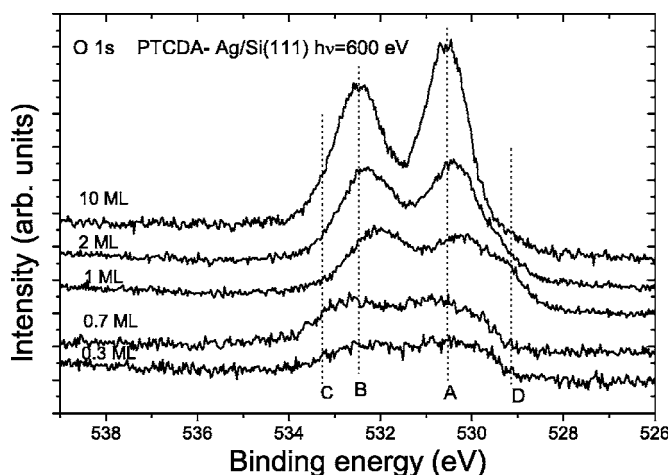


FIG. 5. O 1s core level spectra for PTCDA layers of different thickness on Ag/Si(111)- $\sqrt{3} \times \sqrt{3}$.

2:1 relation based on the stoichiometric relation between the O atoms is caused by a shake-up from the carboxylic peak that overlaps with the anhydride peak.²¹ In the fitted spectrum, there is also a weaker component C at 533.9 eV and a very weak shoulder D at 529.1 eV. The peak C has previously been assigned to a shake-up²¹ but component D has previously not been observed.

Figure 6 shows the peakfits of the O 1s core level at 0.7, 1.0, and 10 ML coverage. The component D at 529.1 eV is strong at low coverage. This component has its strongest relative intensity at 0.3 ML coverage and becomes gradually weaker relative to the main peaks until it is nearly gone for the 10 ML thick film. The energy shifts of the O 1s core levels as a function of coverage are plotted in Fig. 7. The shifts are similar to the shift of the carboxylic related peak in C 1s with the exception of the 1–2 ML coverage region.

D. Carbon 1s NEXAFS

C 1s NEXAFS spectra recorded with different incidence angles for a 10 ML thick film are shown in Fig. 8. An assignment of the peaks for a thick film has previously been done by Taborski *et al.*,²⁵ by comparing NEXAFS data from perylene and perylene derivatives in combination with calculations. The first peak *a* at 283.8 eV is attributed to excitations of the C atoms in the perylene core into the lowest unoccupied molecular orbital (LUMO) with highly directed π orbitals. The most intense peak *b* at 285.2 eV is attributed to excitations of the perylene C atoms into the next three higher orbitals. The peaks *c* and *d* at higher energy 287.4 eV and 288.0 eV can be assigned to excitations of the higher binding energy C atoms in the carboxylic groups. In the PTCDA molecule the LUMO derives from the π^* orbitals which are directed perpendicular to the molecular plane. Due to quantum mechanical selection rules the transition rate between the C 1s core level and π orbitals becomes zero if the electric field vector of the incidence light does not have a component parallel to the π orbitals.²⁶

Comparing the NEXAFS spectra taken from normal (0°) to grazing (70°) incidence in Fig. 8, a dramatic change can

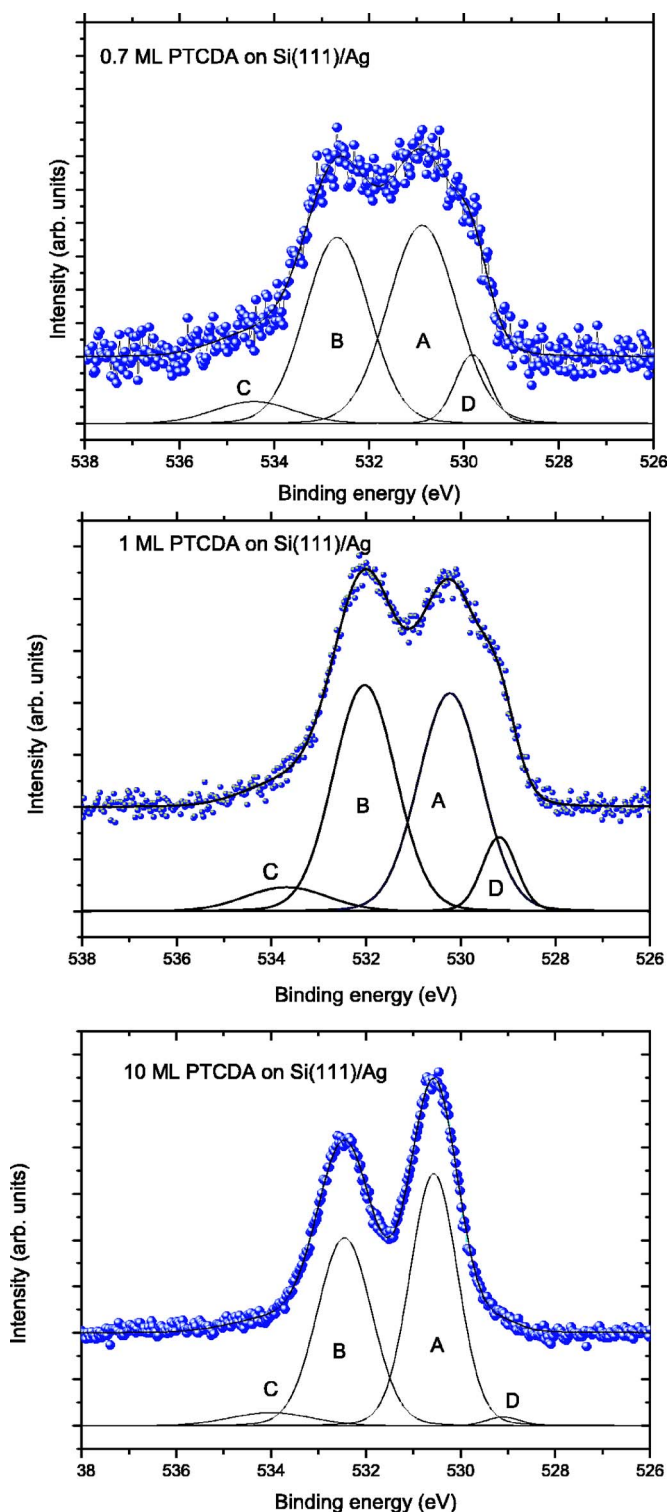


FIG. 6. (Color online) Peakfits of O 1s of 0.7, 1, and 10 ML PTCDA on Si(111)/Ag. Experimental data are shown as points and the fitted lineshape with a continuous line.

be seen. The π resonances below 290 eV have their maxima at grazing incidence while the broad σ resonances above 290 eV show little angle dependence.

The missing π resonances (peaks *a* and *b*) at 283.8 and 285.2 eV in the normal incidence spectrum show that the molecules are oriented flat relative to the substrate²⁵ at 10

TABLE II. Fitting parameters for O 1s components A, B, C, and D. The table shows the energy position ΔE relative peak A in eV, relative integrated intensity I_{rel} and W_G , the FWHM of the Gaussian in eV.

0.7 ML	ΔE	I_{rel}	W_G	1 ML	ΔE	I_{rel}	W_G	2 ML	ΔE	I_{rel}	W_G	10 ML	ΔE	I_{rel}	W_G
A	0	47%	1.72	A	0	42%	1.52	A	0	44%	1.27	A	0	51%	1.13
B	1.80	39%	1.51	B	1.80	44%	1.51	B	1.80	45%	1.46	B	1.88	43%	1.30
C	3.55	5.8%	2.0	C	3.45	6.1%	2.0	C	3.56	4.4%	2.0	C	3.43	4.5%	2.0
D	-1.06	7.4%	0.8	D	-1.04	8.0%	0.8	D	-1.03	6.3%	1.02	D	-1.03	1.3%	0.8

ML. For thick films the NEXAFS spectra look very similar to the corresponding spectra from a thick PTCDA layer of flat lying molecules on Ag(111) (Ref. 27) and on H passivated Si(001).³

Figure 9 shows a comparison of NEXAFS spectra from thin and thick films. For thinner layers the absence of the resonance *a* at 283.8 eV indicates that the LUMO level is affected by the bonding to the substrate and is changed for molecules in the first layer compared to molecules on top in a thicker film. The π^* resonances at grazing incidence for low coverage is quite similar to PTCDA on Ag(111) (Ref. 27) where the first π^* resonance also was missing. The resonance *b* at 285.2 eV is highly angle dependent for submonolayers (not shown), which shows that also the first layer is oriented flat on the surface. It is noteworthy that the changes in NEXAFS spectra as a function of thickness appear in the same range as the major changes of the core level XPS spectra.

E. Low energy electron diffraction

The clean substrate has a strong $\sqrt{3} \times \sqrt{3}$ LEED pattern. This reconstruction can still be seen at higher energies (50–100 eV) when PTCDA is deposited but gets gradually weaker with increasing PTCDA coverage. At 2 ML coverage the intensity is very weak and at 10 ML the $\sqrt{3} \times \sqrt{3}$ LEED spots are completely gone. This indicates a relatively homogeneous coverage of the film, contrary to PTCDA on a H

passivated Si substrate,^{3,28} where the LEED pattern from the substrate could be seen clearly even with a thick PTCDA film deposited.

A LEED pattern from the PTCDA molecules can clearly be seen for electron energies from around 10 up to 35 eV. The pattern is observed already from 0.3 ML coverage at room temperature. Figure 10 shows a LEED pattern recorded from 1.2 ML PTCDA on Ag/Si(111)- $\sqrt{3} \times \sqrt{3}$.²⁹ The pattern is ringlike with two sets of 12 spots *A* and *B* of slightly different intensity. This pattern is similar to the one interpreted as two different phases of herringbonelike ordering of the molecules on Au(111) (Ref. 7) although in that case all diffraction spots were in triangular groups of three spots consisting of the (1,1) (1, $\bar{1}$), and (2,0) spots. In our measurements we have no clear resolution of every spot in the subgroups although we have vague indications that the larger spots *A* is the sum of four smaller spots. Preliminary LEED simulations indicate that more than one phase is needed to explain all the spots. This is consistent with a mix of different square and herringbone phases as recently observed in STM studies.¹⁰ In cases where a single phase was observed as on Ag(111)³⁰ and under some growth conditions for Au(111)⁷ only one set with 12 spots were observed. The 12 symmetrically placed spots are a good indication that there is a sixfold symmetry in our molecular ordering. This arises due to the three different symmetry directions of the substrate and in each of these directions the molecules have two equivalent mirror domains. This also means that the unit cell has a preferred direction to the substrate.

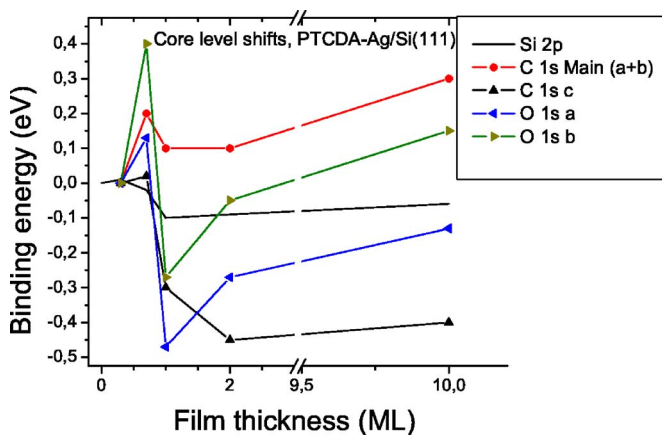


FIG. 7. (Color online) Shifts of the core levels as a function of increasing film thickness. The labels for C 1s are the same as in Fig. 4 and for O 1s as in Fig. 6. The thickness scale has been split in two intervals for clarity.

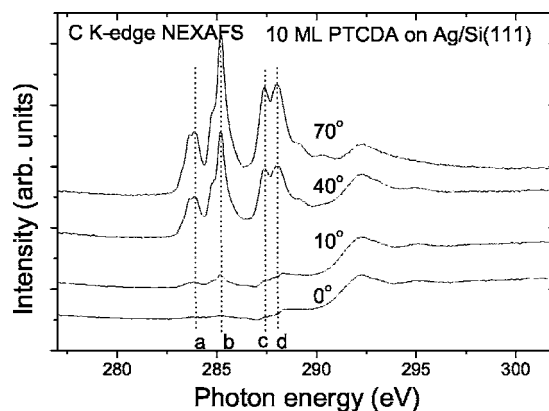


FIG. 8. C 1s NEXAFS spectra of different incidence angles of 10 ML PTCDA on Ag/Si(111)- $\sqrt{3} \times \sqrt{3}$. The angle dependence of peaks *a* and *b* shows that the molecules are oriented flat on the substrate.

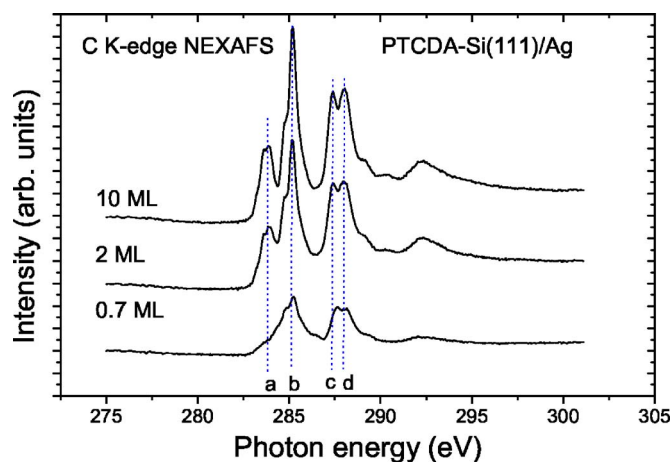


FIG. 9. (Color online) NEXAFS spectra of PTCDA layers with different thickness on the Ag/Si(111)- $\sqrt{3} \times \sqrt{3}$ surface. The incidence angle was 70° .

F. Valence band PES

The VB spectra are dominated by the Ag $4d$ states at 5.9 eV below the Fermi level which makes the interpretation of the PTCDA related data difficult in this energy range. In the spectrum of 10 ML PTCDA on Ag/Si(111)- $\sqrt{3} \times \sqrt{3}$ there are two PTCDA related features at 2.66 eV (HOMO) and 4.34 eV (HOMO-1) binding energy, as seen in Fig. 11. At 2 ML coverage the energy of these peaks are at 2.38 and 3.96 eV and for 1 ML coverage, the energies of these features are shifted to 2.55 and 4.03 eV. For less than one monolayer the spectra show no clear highest occupied molecular orbital (HOMO) peak, which indicates that the orbitals change due to the interaction with the substrate. The HOMO-1 is, however, clearly seen for the 0.7 ML thick film. The modifications of the spectra for submonolayers are similar to the NEXAFS result for the lowest energy resonances,

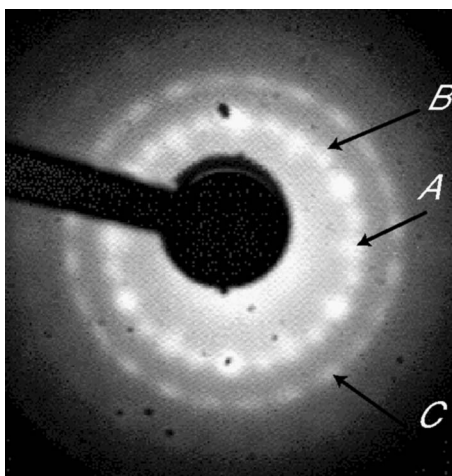


FIG. 10. LEED picture of 1.2 ML PTCDA on Si(111)/Ag with 30 eV electron energy. The spots from the two sets in the inner ring are marked A and B and the spots in the outer ring are marked C. The sample was below room temperature (Ref. 29) but no significant difference was observed compared to room temperature.

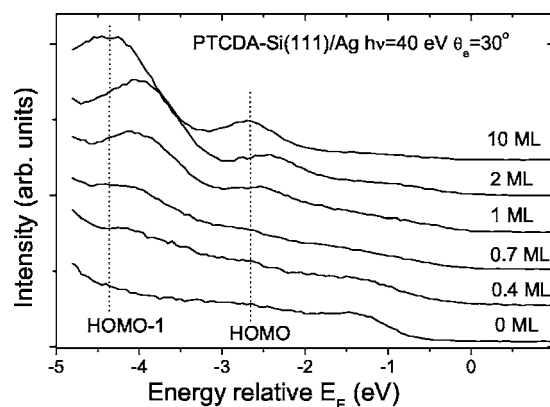


FIG. 11. Valence band spectra of PTCDA layers of different thickness on Ag/Si(111)- $\sqrt{3} \times \sqrt{3}$. HOMO and HOMO-1 are marked. The photon energy was 40 eV and the emission angle 30° .

in the sense that the HOMO, and LUMO are both suppressed at submonolayers. The VB spectra for multilayers also show a clear angle dependence of the peak intensities at 0, 30 and 60 degrees emission angle. The intensity of the resonances is strongest at 30° with the HOMO-1 at 4.3 eV, while it is completely gone at 60° . There is also a shift of the HOMO of 0.23 eV from 2.47 to 2.70 eV when going from 0° to 30° emission angle (spectrum not shown).

The HOMO and HOMO-1 for thick films are known from previous measurements^{4,31} to be at 2.62 and 4.30 eV below the Fermi energy. This is in good agreement with the peak positions in the 10 ML spectrum seen in Fig. 11.

IV. DISCUSSION

There are some significant changes in the results observed in the submonolayer range compared to thicker films. There are changes in the HOMO of the VB spectra as well as LUMO in the NEXAFS measurement. Additional core-level components in the XPS spectra are also observed. Our results show two different interactions between the molecules and the substrate.

The first interaction involves the perylene core of the molecule. This is seen in changes of the HOMO and LUMO levels. According to molecular orbital calculations the HOMO and LUMO are located to the C atoms in the perylene core.³² In the NEXAFS spectra, the LUMO is clearly affected at submonolayer coverage where the first resonance *a* is strongly depressed. The NEXAFS spectra for thinner layers have some similarities to NEXAFS for PTCDA on an Ag(111) surface²⁷ where the excitation to the LUMO is significantly changed, but where the higher excitations as similar to a thick film. When the PTCDA molecules have stronger interactions as in the case with indium deposited on a PTCDA film³³ also the LUMO+N excitations are modified, but in our study this is not the case. The HOMO level has a similar behavior as the LUMO, as it also is strongly suppressed for low coverage, as seen in Fig. 11. The shifts of the HOMO-1 level follows the shifts of the C 1s core level related to the perylene core of the molecule. The HOMO level is modified because of substrate interac-

tion in the first monolayer seen as a shift relative HOMO-1 between 1 and 2 ML. From 2 ML the molecule-molecule interactions dominate and now the HOMO has the same shift as the HOMO-1 and C 1s core levels from 2 to 10 ML thickness.

The shift in the Si 2p core level indicates a 0.11 eV band bending in the substrate, which gives a valence band maximum very close to the Fermi level. With the PTCDA HOMO 2.6 eV below the Fermi level for thicker layers and a transport gap of 3.2 eV (Ref. 34) the substrate valence band and the LUMO could then be relatively close. In the case of PTCDA on Ag(111) there were even indications of a hybridization of the HOMO and LUMO with the Ag 4s band giving a reduction in the gap to 0.4 eV (Ref. 35) and a new peak at 1.7 eV below the Fermi level.^{36,37} We do not see any clear new states in the gap region but the significantly lowered intensity of the HOMO and a tail close to the Fermi level in the valence band spectra on low coverage films, could indicate similar gap states as for the Ag(111) case. The changes in HOMO and LUMO levels would then imply that we have a similar interaction as for Ag(111) where charge is transferred from the surface into the perylene part of the molecule.³⁸

The second interaction is related to the end groups and is seen in the shifts of the core level energies. The C 1s carboxylic peak *c* has similar shifts of binding energy as the O 1s peaks *A* and *B* with the exception of the 1–2 ML coverage range, as seen in Fig. 7. The shift to lower binding energy of the carboxylic group related components when the first monolayer is deposited indicates that there is a charge transfer from the substrate to the end groups of the molecule, giving a more polarized molecule as well as an interface dipole. Above 1 ML film thickness there is a shift back in the O 1s energies indicating that subsequent layers are less affected by this charge transfer. The C 1s component *c* has an opposite shift compared to the O 1s between 1 and 2 ML, indicating a charge transfer due to the dominant molecule-molecule interaction in the carboxylic bond in this range. Above 2 ML thickness all the PTCDA related peaks move to higher binding energy by the same amount. In previous studies a decrease in final state screening from the substrate has been observed³⁹ for increasing film coverage giving higher binding energy. This gives a reasonable explanation also for our shifts above 2 ML coverage.

Additionally the C 1s component *c*, assigned as the main peak in the carboxylic group, is much broader at low coverage compared to higher. The component *d* has a slightly stronger relative intensity on low coverage compared to thicker films, so it is possible that part of its intensity can arise from a shifted component in the carboxylic C atoms similar to the new component in O 1s. Nevertheless, the major part of the intensity in peak *d* clearly has no connection to the substrate interaction, as it is seen also at 10 ML coverage, as well as for PTCDA on the very weakly interacting H passivated Si(001) (Ref. 4) and for thick PTCDA films on Ag(111).²¹

While we cannot fully explain all the interactions in detail we have some suggestions on the origin of the new XPS components. In our study we have changes in the core level spectra for the peaks related to both the carboxylic group and

the perylene core of the molecule. The peak widths at low coverage are higher and there are also some significant shifts in the endgroup related components. There is also an additional C 1s peak *g* at low coverage.

According to the LEED pattern from the molecules the first monolayer appears to be well ordered. The spots also appear to have well ordered orientation relative to the substrate so we have some kind of epitaxial growth of the film. Recent STM studies have shown that two main phases coexist¹⁰ on this surface, which is also consistent with our LEED images. As LEED and STM indicate multiple phases, an explanation to the new XPS components due to the different phases should be considered. The mixed phases may possibly give slight shifts in the binding energies due to differences in molecular ordering and therefore intermolecular interactions.

A more likely explanation is that the new peaks has its origin in substrate interactions, as changes are seen both in the perylene core and the endgroups. With the localized DOS in the substrate and varying adsorption positions, the different atoms in the molecules could be expected to be affected differently by this potential giving shifted core level energies for some atoms. When averaged out over the first monolayer this can be observed as new components as well as a broadening of the peaks.

In the C 1s spectrum a new component *g* is observed at low coverage. This peak has an energy close to the main peak *a* and has a relatively large energy difference of 3.2 eV compared to the carboxylic group related peak. This makes it more likely that this new component has its origin from the atoms in the perylene core of the molecule. The integrated area of the new component is about 15% of the main peak and this rate gets smaller with increasing film thickness already before a full monolayer is reached. Similar results were previously found for pentacene¹⁶ where the XPS spectra at low coverage showed an asymmetry in the C 1s peak. This was reduced to a single peak at higher thickness. This was interpreted as a possible site specific interaction with the substrate at low coverage.

Part of the differences in the submonolayer regime may also have its origin in the fact that defects and nucleation sites at step edges can have a stronger interaction with the molecules as reported in STM studies of C₆₀ on this substrate.¹² The stronger adsorbed molecules may give changes in the binding energies and together with the problems to get good statistics on very low coverage, this makes especially the results on the 0.3 ML coverage a bit more uncertain than for higher coverage. However, as the PTCDA related LEED spots can be seen at 0.3 ML coverage at room temperature a large part of the molecules should be well ordered on the flat terraces.

The peaks in the O 1s spektrum are an indicator for what happens with the end groups. The intensity of the *D* component in Fig. 6 is significantly smaller than the intensity of the two main components *A* and *B* assigned to the two different O atoms in the PTCDA molecule. The intensity of the peak-fitted component *D* corresponds to about 10% of the total intensity at one ML film thickness. The decrease of intensity for component *A* for low coverage compared to thicker films would indicate that it is the carboxylic atoms that have the

strongest interaction with the substrate. This is similar to the findings for PTCDA on Ag(111) where downward bending of the carboxylic O atoms due to charge transfer from the substrate was found giving an increased interaction with the substrate.³⁸ A similar interaction could then explain the shifts in binding energy on low coverage as well as the new component *D*.

For higher coverage of several ML the molecules stack planar to the surface based on the NEXAFS measurements. This is also supported by the angle dependence of the VB spectra. The strong attenuation of the LEED signal of the substrate where the $\sqrt{3} \times \sqrt{3}$ pattern from the substrate almost disappears already for a 2 ML thick film indicates that at least for low coverages there is a complete layered coverage and predominately a layer by layer growth for even thicker layers.

V. CONCLUSIONS

High resolution core level and valence band PES, NEXAFS and LEED have been used to study molecular films of

PTCDA on a Ag/Si(111) $\sqrt{3} \times \sqrt{3}$ substrate. We find evidence of two types of substrate molecule interactions. One with the perylene core of the molecule and one with the end groups. A charge transfer from the surface to the molecules is also indicated. The interactions induce changes in the HOMO and LUMO levels seen in the valence band and NEXAFS measurement. The shifts in the core levels indicate charge transfer. Additional C 1s and O 1s components in the submonolayer range are observed and interpreted as an effect of the localized DOS of the substrate. The molecules stack parallel to the substrate forming a layer by layer growth for thicker films.

ACKNOWLEDGMENTS

The work done here was funded by the Swedish Research Council.

*Electronic address: jorgen.gustafsson@kau.se

- ¹S. R. Forrest, Chem. Rev. (Washington, D.C.) **97**, 1793 (1997).
- ²Y. Hirose, S. R. Forrest, and A. Kahn, Phys. Rev. B **52**, 14040 (1995).
- ³J. B. Gustafsson, E. Moons, S. M. Widstrand, and L. S. O. Johansson, Surf. Sci. **572**, 23 (2004).
- ⁴J. B. Gustafsson, E. Moons, S. M. Widstrand, M. Gurnett, and L. S. O. Johansson, Surf. Sci. **572**, 32 (2004).
- ⁵M. Eremitchenko, J. A. Schaefer, and F. S. Tautz, Nature (London) **425**, 602 (2003).
- ⁶C. Seidel, C. Awater, X. D. Liu, R. Ellerbrake, and H. Fuchs, Surf. Sci. **371**, 123 (1997).
- ⁷S. Mannsfeld, M. Törker, T. Schmitz-Hübsch, F. Sellam, T. Fritz, and K. Leo, Org. Electron. **2**, 121 (2001).
- ⁸R. I. G. Uhrberg, H. M. Zhang, T. Balasubramanian, E. Landemark, and H. W. Yeom, Phys. Rev. B **65**, 081305(R) (2002).
- ⁹N. Sato, T. Nagao, and S. Hasegawa, Surf. Sci. **442**, 65 (1999).
- ¹⁰J. C. Swarbrick, J. Ma, J. A. Theobald, N. S. Oxtoby, J. N. O'Shea, N. R. Champness, and P. H. Beton, J. Phys. Chem. B **109**, 12167 (2005).
- ¹¹M. J. Butcher, J. W. Nolan, M. R. C. Hunt, P. H. Beton, L. Dunsch, P. Kuran, P. Geiorgi, and T. J. S. Dennis, Phys. Rev. B **64**, 195401 (2001).
- ¹²M. D. Upward, P. Moriarty, and P. H. Beton, Phys. Rev. B **56**, R1704 (1997).
- ¹³P. Guaino, A. A. Cafolla, D. Carty, G. Sheerin, and G. Hughes, Surf. Sci. **540**, 107 (2003).
- ¹⁴P. Guaino, D. Carty, G. Hughes, P. Moriarty, and A. A. Cafolla, Appl. Surf. Sci. **212-213**, 537 (2003).
- ¹⁵P. Guaino, A. A. Cafolla, O. McDonald, D. Carty, G. Sheerin, and G. Hughes, J. Phys.: Condens. Matter **15**, 2693 (2003).
- ¹⁶G. Hughes, D. Carty, O. McDonald, and A. A. Cafolla, Surf. Sci. **580**, 167 (2005).
- ¹⁷R. Nyholm, S. Svensson, J. Nordgren, and A. Flodström, Nucl. Instrum. Methods Phys. Res. A **246**, 267 (1995).
- ¹⁸A. Ishizaka and Y. Shiraki, J. Electrochem. Soc. **133**, 666 (1986).

- ¹⁹Unfortunately the monochromator was not calibrated during the experiment. The estimated accuracy is based on a calibration in a later experiment.
- ²⁰Y. Hirose, A. Kahn, V. Aristov, P. Soukiassian, V. Bulovic, and S. R. Forrest, Phys. Rev. B **54**, 13748 (1996).
- ²¹A. Schöll, Z. Zou, M. Jung, T. Schmidt, R. Fink, and E. Umbach, J. Chem. Phys. **121**, 10260 (2004).
- ²²Q. Chen, T. Rada, T. Bitzer, and N. Richardson, Surf. Sci. **547**, 385 (2003).
- ²³P. J. Unwin, D. Onoufriou, J. J. Cox, C. P. A. Mulcahy, and T. S. Jones, Surf. Sci. **482-485**, 1210 (2001).
- ²⁴T. Soubiron, V. Vaurette, J. P. Nys, B. Grandidier, X. Wallart, and S. Stiévenard, Surf. Sci. **581**, 178 (2005).
- ²⁵J. Taborski, P. Väterlein, H. Dietz, U. Zimmermann, and E. Umbach, J. Electron Spectrosc. Relat. Phenom. **75**, 129 (1995).
- ²⁶J. Stöhr, *NEXAFS Spectroscopy* (Springer-Verlag, Berlin, 1992).
- ²⁷E. Umbach, K. Glöcker, and M. Sokolowski, Surf. Sci. **402-404**, 20 (1998).
- ²⁸M. Tengelin-Nilsson, L. Ilver, and J. Kanski, Surf. Sci. **464**, 265 (2000).
- ²⁹LEED measurement was done in a separate (unpublished) experiment with a better LEED optics and camera. The sample was cooled in an attempt to obtain sharper PES peaks and LEED images was taken after deposition but before cooling.
- ³⁰L. Kilian, E. Umbach, and M. Sokolowski, Surf. Sci. **573**, 359 (2004).
- ³¹Y. Azuma, S. Akatsuka, K. K. Okudaira, Y. Harada, and N. Ueno, J. Appl. Phys. **87**, 766 (2000).
- ³²A. K. C. Kendrick and S. R. Forrest, Appl. Surf. Sci. **104/105**, 586 (1996).
- ³³S. Park, T. Kampen, T. Kachel, P. Bressler, W. Braun, and D. R. Zahn, Appl. Surf. Sci. **190**, 376 (2002).
- ³⁴I. Hill, A. Kahn, Z. Soos, and R. Pascal, Jr., Chem. Phys. Lett. **327**, 181 (2000).
- ³⁵F. S. Tautz, M. Eremitchenko, J. A. Schaefer, M. Sokolowski, V. Shklover, and E. Umbach, Phys. Rev. B **65**, 125405 (2002).

- ³⁶M. Jung, U. Vaston, G. Schnitzler, M. Kaiser, J. Papst, T. Porwol, H. J. Freund, and E. Umbach, *J. Mol. Struct.* **293**, 239 (1993).
- ³⁷E. Umbach, C. Seidel, J. Taborski, R. Li, and A. Soukopp, *Phys. Status Solidi B* **192**, 389 (1995).
- ³⁸A. Hauschild, K. Karki, B. C. C. Cowie, M. Rohlfiing, F. S. Tautz, and M. Sokolowski, *Phys. Rev. Lett.* **94**, 036106 (2005).
- ³⁹H. Peisert, M. Knupfer, T. Schwieger, J. M. Auerhammer, M. S. Golden, and J. Fink, *J. Appl. Phys.* **91**, 4872 (2002).